Relationships in the Rotational Barriers of All Group 14 Ethane Congeners H₃X–YH₃ (X, Y = C, Si, Ge, Sn, Pb). Comparisons of ab Initio Pseudopotential and All-Electron Results

Paul v. R. Schleyer,*,[†] Martin Kaupp,[†] Frank Hampel,[†] Matthias Bremer,[†] and Kurt Mislow[‡]

Contribution from the Institut Für Organische Chemie I, Friedrich-Alexander Universität Erlangen–Nürnberg, Henkestrasse 42, 8520 Erlangen, Germany, and Department of Chemistry, Princeton University, Princeton, New Jersey 08544. Received August 9, 1991
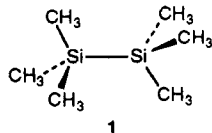
Abstract: The equilibrium structures and energies of the 15 H₃X–YH₃ hydrides, comprised of all possible combinations of group 14 elements, have been calculated in eclipsed and staggered conformations. The relationships between the central bond lengths and the rotational barriers are of particular interest. The barriers decrease but do not vanish at large X–Y separations (e.g. Pb₂H₆). Each of the lighter elements (X = C, Si, Ge) gives a correlation between the barrier heights and the X–Y distances, but the slope decreases down the group. The data for X = Sn, Pb are not as regular in this respect, but all these barriers are small. Most of the X–Y, X–H, and Y–H distances obtained from nonrelativistic all-electron and from quasirelativistic pseudopotential calculations are in good agreement. Only relativistic bond contractions for X or Y = Pb lead to significantly shorter bond distances in the pseudopotential calculations. No systematic effect of relativity on the rotational barriers is found. Stabilizing vinical σ-XH→σ*-YH and σ-YH→σ*-XH interactions in the staggered conformation are responsible for the rotational barriers of the complete series, in agreement with previous studies of ethane. The lower barriers for the heavier species appear to be due to poorer orbital overlap and to increasingly smaller differences between antiperiplanar, synperiplanar, and 120° vicinal overlap. While relativistic bond contraction increases the individual interactions for diplumbane and methylplumbane, it does not appear to affect the rotational barriers. Previous 3-21G(*) results, indicating the rotational barrier in hexamethyldisilane to be very close to that in dislane (ca. 1 kcal/mol), despite the presence of six methyl groups, are confirmed by calculations at higher levels of theory (MP2/6-31G*//6-31G*). When the X–Y distances are even larger, as in most of the group 14 combinations, methyl and similar substituents also should have no significant effect on the rotational barriers.

Introduction

The rotational barriers around single bonds, exemplified by ethane, have been the focus of much experimental and theoretical effort.[1–10] While quite accurate barrier heights can be calculated even at relatively modest levels of theory, the origin of the barriers is still debated.

The early idea that the barrier was due to repulsions among the H's can easily be refuted. Even the simplest ethane congeners, CH₃SiH₃, CH₃GeH₃, and CH₃SnH₃ (data from microwave spectroscopy have been known for some time), exhibit appreciable rotational barriers[11] of 1.7, 1.24, and 0.65 kcal/mol, respectively, even though the vicinal hydrogens are far apart. Indeed, the H⋯H distances must fall in the attractive van der Waals region. We wondered if substantial rotational barriers exist for the other H₃X–YH₃ species, where both X and Y are heavier group 14 elements.

The rotational barrier in hexamethyldisilane (**1**) served as another impetus for this work. Knowledge of the magnitude of such barriers is important for the parametrization of empirical

1

force fields, but molecular mechanics have yielded quite different results. Mislow et al.[12] reported a calculated barrier of 1.05 kcal/mol in 1977 whereas Allinger,[13] using a modified MM2 force field, reported the much higher value of 5.77 kcal/mol in 1988. The latter was in apparently good agreement with the 5.7-kcal/mol barrier deduced from solid-state NMR data.[14] Ab initio calculations are clearly capable of resolving this discrepancy. Indeed, during the course of our own work, Profeta, Unwalla, and Cartledge[15] reported results on a comprehensive set of Si–C

barriers involving a number of methyl-substituted silanes. Their results, which were employed to help reparametrize empirical force fields for silicon, are much more consistent with the data presented initially by Mislow[12] and later by Damewood and West[16] for poly(dimethylsilane)s. In particular, a surprising prediction by Mislow[12] was supported. Despite the presence of the six methyl groups, the rotational barrier of Me₃Si–SiMe₃ (**1**) is not higher than that of the parent disilane H₃Si–SiH₃! However, Profeta et al.'s ab initio calculations on **1** were only carried out with the relatively modest 3-21G(*) basis set,[15] and the effect of correlation energy on the rotational barrier of this molecule was not assessed. As Wiberg[17] has shown that electron correlation effects can be

(1) For a review of experimental and theoretical studies of the ethane barrier up to the early 1980's, see: Pitzer, R. M. *Acc. Chem. Res.* **1983**, *16*, 207.

(2) Sovers, O. J.; Kern, C. W.; Pitzer, R. M.; Karplus, M. *J. Chem. Phys.* **1968**, *49*, 2592.

(3) Whangbo, M.-H; Schlegel, H. B.; Wolfe, S. *J. Am. Chem. Soc.* **1977**, *99*, 1296.

(4) Musso, G. F.; Magnasco, V. *J. Chem. Soc., Faraday Trans. 2* **1982**, *78*, 1609.

(5) England, W.; Gordon, M. S. *J. Am. Chem. Soc.* **1971**, *93*, 4649.

(6) Corcoran, C. T.; Weinhold, F. *J. Chem. Phys.* **1980**, *72*, 2866.

(7) Brunck, T. K.; Weinhold, F. *J. Am. Chem. Soc.* **1979**, *101*, 1700.

(8) Surján, P. R. *Croat. Chim. Acta* **1983**, *56*, 289.

(9) Bader, R. F. W.; Cheeseman, J. R.; Laidig, K. E.; Wiberg, K. B.; Breneman, C. *J. Am. Chem. Soc.* **1990**, *112*, 6530.

(10) Reed, A. E.; Weinhold, F. A. *Isr. J. Chem.* In press.

(11) (a) Harmony, M. D.; Laurie, V. W.; Kuczkowski, R. L.; Schwendeman, R. H.; Ramsay, D. A.; Lovas, F. J.; Lafferty, W. J.; Maki, A. G. *J. Phys. Chem. Ref. Data* **1979**, *8*, 619. (b) Pfeiffer, M.; Spangenberg, H.-J. *Z. Phys. Chem.* **1966**, *232*, 47. (c) Durig, J. R.; Whang, C. M.; Attia, G. M.; Li, Y. S. *J. Mol. Spectrosc.* **1984**, *108*, 240. (d) Pouchan, C.; Lespes, G.; Dargelos, A. *J. Phys. Chem.* **1988**, *92*, 28.

(12) Mislow, K.; Stackhouse, J.; Hummel, J. P. *Tetrahedron* **1977**, *33*, 1925.

(13) Frierson, M. R.; Imam, M. R.; Zalkow, V. B.; Allinger, N. L. *J. Org. Chem.* **1988**, *53*, 5248.

(14) Yukitoshi, T.; Suga, H.; Siki, S.; Itoh, J. *J. Phys. Soc. Jpn.* **1957**, *12*, 506.

(15) Profeta, S., Jr.; Unwalla, R. J.; Cartledge, F. K. *J. Comp. Chem.* **1989**, *10*, 99.

(16) Damewood J. R., Jr.; West, R. J. *Macromolecules* **1985**, *18*, 159.

[†] Universität Erlangen–Nürnberg.
[‡] Princeton University.

significant in branched systems, it was desirable to examine **1** at higher theoretical levels. If the methyl groups have no significant influence on the magnitude of the rotational barrier of **1**, they should hardly be important in the lower group 14 congeners.

The additional principal questions we wished to answer are as follows: 1. What are the rotational barriers for the entire set of fifteen molecular combinations H_3X-YH_3 (X, Y = C, Si, Ge, Sn, Pb)? 2. Are there relationships between the central bond lengths of these molecules and the rotational barriers? 3. What are the origins of the single bond rotation barriers? Do these change when heavier group 14 elements are involved? 4. How do the results from pseudopotential and all-electron calculations compare? (This is of importance for future ab initio calculations of larger systems containing the heavier group 14 elements).

Besides Si_2H_6,[18] prior experimental and computational examinations of rotational barriers for these molecules have largely been confined to the CH_3-XH_3 derivatives.[11,19,20] Some structural data also are available for Ge_2H_6 and for $H_3Si-GeH_3$.[11,21,22] The other members of the H_3X-YH_3 set are unknown experimentally and have not been studied by ab initio calculations before. X–H and X–C distances for XH_4 and $X(CH_3)_4$ (X = C, Si, Ge, Sn, Pb) are available from relativistic ab initio studies and experiment,[23] and may be compared to the corresponding values for our set of molecules. Attention is called to pertinent reviews on rotational barriers[1-10] and on the performance of various standard levels of ab initio theory.[19]

Computational Details

The geometries were fully optimized at the Hartree–Fock level of theory, using standard gradient optimization techniques. The CADPAC program package[24] has been used for the all-electron calculations (six Cartesian d-functions implied) and Gaussian 88[25] for the pseudopotential calculations (five d-functions). The built-in default thresholds of the two programs were used for wave function and gradient convergence. Natural population analyses (NPA)[26] have been confined to the pseudopotential calculations and employed Reed's Gaussian 88 adaptation of the NBO program. (See ref 26c for an excellent review of the NPA/NBO analysis of wave functions.) The usefulness of the NBO method to analyze deviations from ideal Lewis structures in molecules is well-documented by numerous studies on hyperconjugation, anomeric effects, hypervalency, etc..[26,27]

Except for the more detailed study of disilane, hexamethyldisilane (**1**), and hexamethylethane (see section D), our all-electron calculations employed the 3-21G(D,P) basis sets for C, Si, and H.[28] For Ge, Sn, and Pb, basis sets of Huzinaga et al.[29] have been used in a split-valence

(17) Wiberg, K. B.; Murcko, M. A. *J. Am. Chem. Soc.* **1988**, *110*, 8029.

(18) Beagley, B.; Conrad, A. R.; Freeman, J. M.; Monaghan, J. J.; Norton, B. G.; Halywell, G. C. *J. Mol. Struct.* **1972**, *11*, 371.

(19) Hehre, W. J.; Radom, L.; Schleyer, P. v. R.; Pople, J. A. *Ab Initio Molecular Orbital Theory*; Wiley: New York, 1986.

(20) (a) Callomon, J. H.; Hirota, E.; Kuchitsu, K.; Lafferty, W. J.; Maki, A. G.; Pote, C. S. *Structure Data on Free Polyatomic Molecules*; Springer-Verlag: Berlin, 1976; Landolt-Börnstein, New Series, Group II, Vol. 7. (b) Callomon, J. H.; Hirota, E.; Iijima, T.; Kuchitsu, K.; Lafferty, W. J. *Structure Data on Free Polyatomic Molecules*; Springer-Verlag: Berlin, 1987; Landolt-Börnstein, New Series, Group II, Vol. 15. (supplement to Vol. 7).

(21) Dobbs, K. D.; Hehre, W. J. *J. Comp. Chem.* **1985**, *7*, 359.

(22) Chase, M. W.; Curnutt, J. L.; Downey, J. R.; McDonald, R. A.; Syverud, A. N.; Valenzuela, E. A. *J. Phys. Chem. Ref. Data* **1982**, *11*, 695.

(23) Almlöf, J.; Faegri K., Jr. *Theor. Chim. Acta* **1986**, *69*, 438. The paper includes various references to experimental structural data.

(24) Amos, R. D.; Rice, J. A. CADPAC; Issue 4; Cambridge, 1987.

(25) Gaussian 88: Frisch, M. J.; Head-Gordon, M.; Schlegel, H. B.; Raghavachari, K.; Binkley, J. S.; Gonzalez, C.; DeFrees, D. J.; Fox, D. J.; Whiteside, R. A.; Seeger, R.; Melius, C. F.; Baker, J.; Kahn, L. R.; Stewart, J. J. P.; Fluder, E. M.; Topiol, S.; Pople, J. A., Gaussian, Inc.: Pittsburgh, PA.

(26) (a) Reed, A. E.; Weinstock, R. B.; Weinhold, F. *J. Chem. Phys.* **1985**, *83*, 735. (b) Reed, A. E.; Weinhold, F. *J. Chem. Phys.* **1985**, *83*, 1736. (c) Reed, A. E.; Curtiss, L. A.; Weinhold, F. *Chem. Rev.* **1988**, *88*, 899.

(27) For some recent applications see the following and numerous references cited therein: Reed, A. E.; Weinhold, F. *J. Am. Chem. Soc.* **1986**, *108*, 3586. Reed, A. E.; Schleyer, P. v. R. *J. Am. Chem. Soc.* **1987**, *109*, 7362. Schleyer, P. v. R.; Reed, A. E. *J. Am. Chem. Soc.* **1988**, *110*, 4453. Reed, A. E.; Schleyer, P. v. R. *J. Am. Chem. Soc.* **1990**, *112*, 1434.

(28) Binkley, J. S.; Pople, J. A.; Hehre, V. J. *J. Am. Chem. Soc.* **1980**, *102*, 939. Gordon, M. S.; Binkley, J. S.; Pople, J. A.; Pietro, W. J.; Hehre, W. J. *J. Am. Chem. Soc.* **1982**, *104*, 2797. Pietro, W. J.; Francl, M. M.; Hehre, W. J.; DeFrees, D. J.; Pople, J. A; Binkley, J. S. *J. Am. Chem. Soc.* **1982**, *104*, 5039.

Table I. X–Y Distances, R (Å), and Rotational Barriers, ΔE_{rot} (kcal/mol), for H_3X-YH_3 Molecules (X, Y = C, Si, Ge, Sn, Pb)

		all-electron calculations			pseudopotential calculations		
X	Y	$R_{st}{}^a$	$R_{ec}{}^a$	ΔE_{rot}	$R_{st}{}^a$	$R_{ec}{}^a$	ΔE_{rot}
C	C	1.542	1.556	2.751	1.526	1.539	2.776
C	Si	1.883	1.893	1.422	1.883	1.893	1.388
C	Ge	1.990	1.999	1.104	1.996	2.004	0.986
C	Sn	2.188	2.193	0.498	2.178	2.184	0.520
C	Pb	2.275	2.278	0.204	2.242	2.246	0.321
Si	Si	2.342	2.355	0.949	2.355	2.364	0.823
Si	Ge	2.409	2.420	0.613	2.425	2.433	0.682
Si	Sn	2.610	2.617	0.581	2.610	2.616	0.476
Si	Pb	2.695	2.701	0.486	2.640	2.645	0.358
Ge	Ge	2.499	2.513	0.664	2.499	2.506	0.528
Ge	Sn	2.662	2.667	0.445	2.669	2.675	0.408
Ge	Pb	2.741	2.745	0.395	2.705	2.709	0.315
Sn	Sn	2.850	2.855	0.412	2.843	2.847	0.350
Sn	Pb	2.928	2.930	0.309	2.869	2.873	0.286
Pb	Pb	3.012	3.015	0.214	2.897	2.900	0.230

$^a R_{st}$ and R_{ec} are the X–Y distances for the staggered and eclipsed conformations, respectively.

contraction, augmented by one d-polarization function. The resulting contraction pattern is (43321/4321/41*), (433321/43321/431*), and (4322211/422211/4221*/4) for Ge, Sn, and Pb, respectively.

For the valence-only calculations, quasirelativistic 4-valence-electron MEFIT (multielectron fit) pseudopotentials were adopted for the group 14 elements.[30,31] This allows the inclusion of the most important relativistic effects, which may be significant for compounds of the heavier elements. For some of the lead derivatives we also used a nonrelativistic lead pseudopotential.[31] Comparison between calculations employing the quasirelativistic and the nonrelativistic lead pseudopotential allows the magnitude of relativistic effects to be evaluated. The 4s4p-valence basis sets[30,31] were contracted to DZ (31/31) and augmented by one set of d-type polarization function.[28,29] The (4s1p)/[2s1p] hydrogen basis set of Dunning and Hay[32] was employed for the pseudopotential calculations. Hence, the description of the valence space is somewhat more extensive than that used for the all-electron calculations.

For the comparison of the unsubstituted and the hexamethyl-substituted ethanes and silanes, we employed various standard basis sets[19] and Møller–Plesset perturbation theory (MP2, MP4) for the electron-correlation corrections. The standard notations for these levels of theory are, e.g., MP2/6-31G*//6-31G*, which indicates an MP2 single point calculation with the polarized split valence 6-31G* basis set using the geometry optimized at the Hartree–Fock level with the same basis (see ref 19 for further details).

Results and Discussion

We first establish the reliability of the computational methods employed. Readers who are more interested in the chemical results may wish to skip section A.

A. Comparison of Results from All-Electron and Pseudopotential Calculations. Table I summarizes the X–Y distances, both for staggered and eclipsed conformations (R_{st}, R_{ec}), and the rotational barriers (ΔE_{rot}) obtained from all-electron and pseudopotential calculations for the complete set of 15 H_3X-YH_3 molecules. Table II compares our data with earlier experimental and theoretical results.

In most cases the X–Y distances obtained from all-electron 3-21G(D,P) calculations agree well with the pseudopotential results. The slight overestimation of the C–C separation in the all-electron calculation for ethane is due to the well-known deficiencies of this 3-21G basis set[19] (the 6-31G* value is quite good, Table II). With lead compounds, the quasirelativistic pseudopotential calculations give Pb–Y bonds substantially shorter than the all-electron results. Relativistic bond contractions for Pb

(29) *Gaussian Basis Sets for Molecular Calculations*; Huzinaga, S., Ed.; Elsevier: New York, 1984.

(30) Küchle, W.; Bergner, A.; Dolg, M.; Stoll, H.; Preuss, H. To be submitted for publication.

(31) Küchle, W.; Dolg, M.; Stoll, H.; Preuss, H. *Mol. Phys.* **1991**, *74*, 1245.

(32) Dunning, T. H.; Hay, H. In *Methods of Electronic Structure Theory* (Modern Theoretical Chemistry, Vol. 3); Schaefer H. F., III, Ed.; Plenum Press: 1977; p. 1ff.

Table II. Comparison of X–Y Distances and Rotational Barriers with Previous Calculations and Experiments[a]

species (barrier)	this work		previous calculations			experiment
	ae[b]	PP[c]	3-21G[(*)]	6-31G*	others	
H$_3$C–CH$_3$	1.542	1.526	1.542[d]	1.527[d]	1.527[d,e]	1.531[d]
(barrier)	(2.75)	(2.78)	(2.7)[d]	(2.9)[d]		(2.9)[d]
H$_3$C–SiH$_3$	1.883	1.883	1.883[d]	1.888[d]	1.880[e]	1.864[f]
(barrier)	(1.42)	(1.39)			(1.40)[e]	(1.7)[j]
H$_3$C–GeH$_3$	1.990	1.996	1.979[g]			1.945[f]
(barrier)	(1.10)	(0.99)				(1.24)[j]
H$_3$Si–SiH$_3$	2.342	2.355	2.342[d]	2.353[d]	2.338[d,e]	2.327[f]
(barrier)	(0.95)	(0.82)		0.95	1.09[e]	(1.22)[h]
H$_3$Si–GeH$_3$	2.409	2.425	2.399[g]			2.357[f]
(barrier)	(0.61)	(0.68)				
H$_3$Ge–GeH$_3$	2.499	2.499	2.447[g]			2.403[f]
(barrier)	(0.66)	(0.53)				
H$_3$C–SnH$_3$	2.188	2.178			2.108, 2.148[i]	2.140[f]
(barrier)	(0.50)	(0.52)			(0.5–0.6)[i]	(ca. 0.6)[j]

[a] X–Y distances for the staggered conformation are given in Å and rotational barriers (in parentheses) in kcal/mol. [b] All-electron calculations. [c] Pseudopotential calculations. [d] Summarized in ref 19. [e] MP2(full)/6-31G*//MP2(full)/6-31G*. [f] Reference 20. [g] 3-21G[(*)]-type basis sets for third- and fourth-row elements by Dobbs and Hehre (ref 21). [h] Reference 18. [i] Relativistic pseudopotential calculations by Pouchan et al. (ref 11d). SCF and MP2 results. [j] Reference 11.

Table III. Comparison of X–H and X–C Distances (Å) for H$_3$C–XH$_3$ with Corresponding Data for XH$_4$ and X(CH$_3$)$_4$[a]

	X–H distance			X–C distance		
	H$_3$C–XH$_3$[b]	XH$_4$		H$_3$C–XH$_3$[b]	X(CH$_3$)$_4$	
X	PP (ae)	theor[a]	exp[c]	PP (ae)	theor[a]	exp[c]
C	1.083 (1.084)	1.083	1.086	1.526 (1.541)	1.540	1.539
Si	1.477 (1.477)	1.482	1.481	1.883 (1.883)	1.902	1.875
Ge	1.540 (1.560)	1.521	1.527	1.996 (1.990)	1.970	1.980
Sn	1.714 (1.739)	1.705	1.701	2.178 (2.188)	2.150	2.143
Pb	1.744 (1.825)	1.703		2.242 (2.275)	2.247	2.238

[a] Results for XH$_4$ and X(CH$_3$)$_4$ from all-electron calculations with Breit–Hamiltonian and first-order perturbational treatment of relativistic effects (see ref 23). [b] This work, pseudopotential calculations (all-electron results are given in parentheses). [c] Experimental data cited at ref 23 are given in parentheses.

compounds are well-established.[23,33] The magnitude of the bond contraction depends on the stretching force constant. This accounts for the very large change in distance of the weak Pb–Pb bond in diplumbane (H$_3$Sn–PbH$_3$ is similar). The differences between the all-electron and the pseudopotential X–Y distances given for the lead compounds may even be underestimated due to a bond shortening caused by basis set superposition errors in the all-electron case. This is indicated by our results for diplumbane (R_{st} = 3.061 Å, R_{ec} = 3.066 Å, ΔE_{rot} = 0.313 kcal/mol) obtained with a nonrelativistic lead pseudopotential.[31] For methylplumbane, the nonrelativistic pseudopotential values (R_{st} = 2.273 Å, R_{ec} = 2.277 Å, ΔE_{rot} = 0.363 kcal/mol) agree much better with the all-electron results (cf. Table I). Obviously it is important to include relativistic effects for the distances in the lead compounds.

Table III compares the X–H and X–C distances obtained for the H$_3$C–XH$_3$ molecules with the corresponding distances in XH$_4$ and X(CH$_3$)$_4$ given by the relativistic all-electron calculations of Almlöf and Faegri, as well as from experiment.[23] As with the X–C and the other X–Y distances (cf. Table I), relativistic effects on the X–H distances are significant when X, Y = Pb. The agreement between our pseudopotential calculations (for H$_3$C–XH$_3$) and the results of Almlöf and Faegri generally is good (except for deviations for the Pb–H distance in methylplumbane). This indicates a high degree of transferability of the X–H and X–C separations between the different sets of molecules. The agreement between the pseudopotential results for H$_3$C–XH$_3$ and the available experimental distances for XH$_4$ and X(CH$_3$)$_4$ species also is noteworthy.

(33) For a recent review of relativistic effects on molecular structure, including lead compounds, see: Pyykkö, P. *Chem. Rev.* **1988**, *88*, 563.

(34) Beagley, B.; Monaghan, J. J.; Hewitt, T. G. *J. Mol. Struct.* **1971**, *8*, 401.

(35) Bartell, L. S.; Boates, T. L. *J. Mol. Struct.* **1976**, *32*, 397.

The H–X–Y angles for all species lie within a narrow range, ca. 110–112°. The angles in the eclipsed conformations are ca. 0.1–0.5° larger than those in the staggered ones. However, no systematic trend in bond angles, e.g. in relationship to the barrier heights, could be discerned. A complete table of the angles obtained from the pseudopotential calculations is available as supplementary material.

The rotational barriers obtained from pseudopotential and all-electron calculations (cf. Table I) generally agree within ca. 0.15 kcal/mol, even when X, Y = Pb. No systematic patterns in the deviations are apparent. Hence, relativistic effects do not appear to influence the barriers. This is surprising, as the considerably shorter distances in the quasirelativistic valence-only calculations for the lead compounds might have led to larger barriers. We will discuss this matter further in section C.

Quasirelativistic pseudopotentials afford an efficient means to calculate geometries and conformational energies of heavier group 14 compounds. The savings in computational time compared to all-electron calculations of similar quality, and the convenient possibility of including relativistic effects (which are important at least for the lead compounds), makes pseudopotentials the method of choice for ab initio calculations on larger molecules. Moreover, we can analyze the results obtained for all the H$_3$X–YH$_3$ species with basis sets of the same size, and the molecules can be treated as 14-electron systems throughout. Hence, our further discussion is based on the pseudopotential results.

B. Relations between Central Bond Length and Rotational Barrier. Figure 1a shows a composite plot of the rotational barriers against the central bond lengths for all H$_3$X–YH$_3$ molecules. While the general decrease in the barriers at larger distances is apparent, there is no clear-cut correlation encompassing the complete data set. Figure 1b shows the improvement when symmetrical H$_3$X–XH$_3$ species are selected. But better correlations are found when X is fixed to C, Si, or Ge and only Y varied (cf. Figure 1c–e). For X = Sn, Pb, the barriers are so small (0.2–0.5 kcal/mol) that plots (cf. Figure 1f,g) of the variations with Y, and the scattering of the points, are not very significant. The accuracy of the calculations can hardly be expected to be better than 0.1 kcal/mol. Generally, the slopes of the regression lines in Figure 1c–g decrease along the series X = C, Si, Ge, Sn, Pb. For X = C there is a strong dependence of the rotational barrier on the nature of Y, but for X = Pb the barrier is almost independent of Y. While the rotational barriers for the heavier species generally are small, they still appear to be significant, even for Pb$_2$H$_6$.

C. Natural Bond Orbital Analysis of the Rotational Barriers. Many possible contributions to the rotational barrier in ethane have been shown to be negligible or could be ruled out completely (see, e.g., ref 1). In recent years the discussion of the origin of single bond barriers has centered on the dominance of attractive delocalization[5-7] vs repulsive overlap interactions.[1-4] Is the
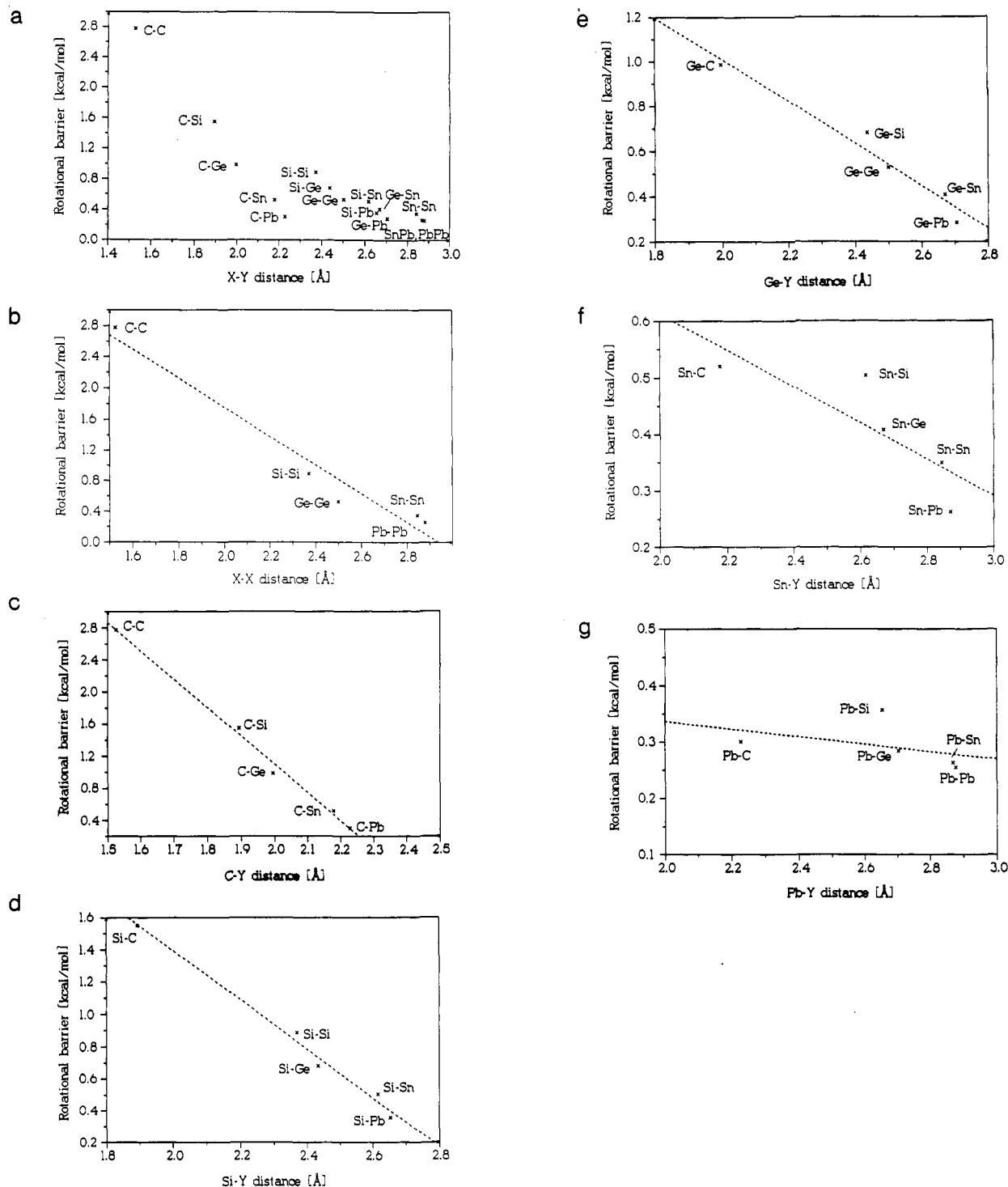
6794 *J. Am. Chem. Soc., Vol. 114, No. 17, 1992*

Schleyer et al.

Figure 1. (a) Composite rotational barrier versus X–Y distance plot for all the H_3X–YH_3 species (X, Y = C, Si, Ge, Sn, Pb). (b) Rotational barrier versus X–X distance plot for H_3X–XH_3 species (X = C, Si, Ge, Sn, Pb). (c) Rotational barrier versus C–Y distance plot for H_3C–YH_3 species (Y = C, Si, Ge, Sn, Pb). (d) Rotational barrier versus Si–Y distance plot for H_3Si–YH_3 species (Y = C, Si, Ge, Sn, Pb). (Note the change in scale from parts a–c.) (e) Rotational barrier versus Ge–Y distance plot for all possible H_3Ge–YH_3 species (Y = C, Si, Ge, Sn, Pb). (Note the reduction in scale from parts a–d.) (f) Rotational barrier versus Sn–Y distance plot for H_3Sn–YH_3 species (Y = C, Si, Ge, Sn, Pb). (Note the further reduction in scale from parts a–e.) (g) Rotational barrier versus Pb–Y distance plot for H_3Pb–YH_3 species (Y = C, Si, Ge, Sn, Pb). There is hardly any difference in these barriers.

staggered ethane favored because it is stabilized by attractive forces relative to the eclipsed conformation or is the later destabilized relative to the former by exchange repulsions? Remarkably, the answer to this question provided by bond orbital or localized MO schemes appears to depend strongly on whether these orbitals are orthogonal or not.[6,8] The use of orthogonal orbitals emphasizes the attractive contributions from delocalization.[6,7] In contrast, schemes employing nonorthogonal orbitals attribute the rotational barrier in ethane mainly to repulsive overlap terms.[1–4] Surján has expressed the view[8] that this apparent discrepancy depends only

on the mathematical framework employed and does not represent any physical difference. The interpretation of the barrier also is influenced by the use of the rigid rotation approximation vs the use of fully optimized geometries for the eclipsed and staggered conformations.[6,9]

We will follow the natural bond orbital (NBO) approach employed by Weinhold and co-workers.[6,7,10,26] As the NBOs are orthogonal, we focus on the attractive delocalization effects. This choice is supported by the conclusions of Bader and co-workers,[9] who employed the (orbital-independent) "atoms-in-molecules"

Table IV. Vicinal $\sigma CH \rightarrow \sigma^* YH$ and $\sigma YH \rightarrow \sigma^* CH$ Delocalizations for $H_3C\text{-}YH_3$ Molecules; Analysis of the NBO–Fock Matrix by Second-Order Perturbation Theory

| Y | | staggered | | | | eclipsed | | | ΔE | ΔE_{rot} |
		CH→YH*	YH→CH*	total		CH→YH*	YH→CH*	total		
C	anti	3 × 3.46	3 × 3.46	23.16	syn	3 × 0.98	3 × 0.98	17.40	5.76	2.78
	gauche	6 × 0.20	6 × 0.20		120°	6 × 0.96	6 × 0.96			
Si	anti	3 × 1.40	3 × 1.33	9.99	syn	3 × 0.87	3 × 0.42	8.07	1.92	1.39
	gauche	6 × 0.20	6 × 0.10		120°	6 × 0.35	6 × 0.35			
Ge	anti	3 × 0.88	3 × 0.84	6.63	syn	3 × 0.57	3 × 0.60	5.91	0.72	0.99
	gauche	6 × 0.15	6 × 0.19		120°	6 × 0.21	6 × 0.19			
Sn	anti	3 × 0.71	3 × 0.45	5.04	syn	3 × 0.38	3 × 0.51	4.35	0.69	0.52
	gauche	6 × 0.08	6 × 0.18		120°	6 × 0.20	6 × 0.08			
Pb[a]	anti	3 × 0.75	3 × 0.55	4.86	syn	3 × 0.28	3 × 0.42	4.32	0.54	0.32
	gauche	6 × 0.03	6 × 0.13		120°	6 × 0.24	6 × 0.13			
Pb[b]	anti	3 × 0.66	3 × 0.37	4.23	syn	3 × 0.30	3 × 0.39	3.69	0.54	0.32
	gauche	6 × 0.06	6 × 0.13		120°	6 × 0.20	6 × 0.07			

[a] Quasirelativistic lead pseudopotential. [b] Nonrelativistic lead pseudopotential.

Table V. Vicinal $\sigma XH \rightarrow \sigma^* XH$ Delocalizations for Symmetrical $H_3X\text{-}XH_3$ Molecules; Analysis of the NBO–Fock Matrix by Second-Order Perturbation Theory

X		staggered	total		eclipsed	total	ΔE	ΔE_{rot}
C	anti	6 × 3.46	23.16	syn	6 × 0.98	17.40	5.76	2.78
	gauche	12 × 0.20		120°	12 × 0.96			
Si	anti	6 × 1.19	8.22	syn	6 × 0.50	7.32	0.90	0.82
	gauche	12 × 0.09		120°	12 × 0.36			
Ge	anti	6 × 0.88	7.08	syn	6 × 0.61	6.54	0.52	0.53
	gauche	12 × 0.15		120°	12 × 0.24			
Sn	anti	6 × 0.82	5.88	syn	6 × 0.41	5.58	0.30	0.35
	gauche	12 × 0.08		120°	12 × 0.26			
Pb[a]	anti	6 × 1.29	8.46	syn	6 × 0.47	8.22	0.24	0.23
	gauche	12 × 0.06		120°	12 × 0.45			
Pb[b]	anti	6 × 0.62	4.32	syn	6 × 0.28	4.08	0.24	0.31
	gauche	12 × 0.05		120°	12 × 0.20			

[a] Quasirelativistic lead pseudopotential. [b] Nonrelativistic lead pseudopotential.

approach to the analysis of the problem. Is the origin of the smaller, but still significant, rotational barriers for the heavier group 14 ethane congeners the same as that for the parent ethane? How can we rationalize the observed trends for the barrier heights? As we are mainly interested in relative contributions and not in a more quantitative treatment, we did not perform Fock matrix deletion analyses[26] (which, for the complete set of molecules, would be beyond the scope of this study). Instead, the nondiagonal elements of the Fock matrix in the NBO basis are analyzed by second-order perturbation theory. This provides information concerning the interactions between the strictly localized almost fully occupied bonding NBOs and the almost empty "Rydberg-type" or antibonding NBOs. These interactions result in deviations from the ideal Lewis structure.[26] Since the energy contributions are relatively small (up to ca. 6 kcal/mol), such second-order estimates can be expected to agree reasonably well with the Fock matrix deletion values.[26] NBO analysis attributes the rotational barrier around the C–C single bond in ethane to the stabilizing hyperconjugation interactions between vicinal σ-CH and σ^*-C'H' NBOs.[6,7,10,26] These are optimal for the antiperiplanar CH bonds in the staggered conformation. We have now analyzed the important interactions for the heavier homologues similarly by decomposing the pseudopotential wave functions. However, the very small energy differences for the heavier species (cf. Table I) complicate a more quantitative study.

In addition to $\sigma HX \rightarrow \sigma^* HY$ (and to $\sigma HY \rightarrow \sigma^* HX$) hyperconjugation, other orbital interactions in the perturbation theoretical analysis, such as geminal $\sigma XH \rightarrow \sigma^* XH$, $\sigma XH \rightarrow \sigma^* XY$, and $\sigma XY \rightarrow \sigma^* XH$ terms, become large for the heavier $H_3X\text{-}YH_3$ molecules (values of ca. 6 kcal/mol are found for X or Y = Pb). However, the orientational dependence of these other interactions (and therefore their influence on the rotational barriers) remains very small. Hence, the energy terms resulting from vicinal

$\sigma HX \rightarrow \sigma^* HY$ (and $\sigma HY \rightarrow \sigma^* HX$) interactions are the only contributions that favor the staggered conformation.

Tables IV and V summarize the second-order vicinal interactions for the $H_3C\text{-}YH_3$ and the symmetrical $H_3X\text{-}XH_3$ molecules, respectively. In both tables, the next to last column (ΔE) gives the net stabilization obtained by subtracting the total vicinal delocalization for the eclipsed conformation from that for the staggered conformation. The correlation with the rotational barriers (last column, ΔE_{rot}) is reasonable in both Tables IV and V. The ΔE values are too large for ethane and methylsilane, but these are the cases with the largest individual contributions. (The error of a perturbation theoretical analysis is expected to be related to the magnitude of the perturbation studied.) The sum of the vicinal contributions (for each conformer) decreases along the series X, Y = C, Si, Ge, Sn. This decrease must be due to poorer orbital overlap, since the orbital energy differences (i.e. the denominator of the perturbational interaction-energy expression) are *smaller* with the heavier and less electronegative elements. The contour plots in Figure 2 provide graphical comparisons of how well the relevant NONBOs (the nonorthogonal NBOs obtained prior to interatomic orthogonalization[26]) for methylstannane, ethane, and distannane overlap with each other: Both $\sigma CH \rightarrow \sigma^* SnH$ and $\sigma SnH \rightarrow \sigma^* CH$ overlap in methylstannane (Figure 2a,b) is significantly less favorable than the $\sigma CH \rightarrow \sigma^* CH$ overlap in ethane (Figure 2c). In particular, the hyperconjugative donor ability of the σSnH NONBO is reduced significantly by its polarization toward hydrogen (cf. the second-order interactions in Table IV). The $\sigma SnH \rightarrow \sigma^* SnH$ overlap for distannane is even less (cf. Figure 2d).

Such antiperiplanar contributions to methylplumbane and particularly to diplumbane are larger in the quasirelativistic pseudopotential calculations than those for the corresponding Sn compounds. For Pb_2H_6, even the total delocalization energy
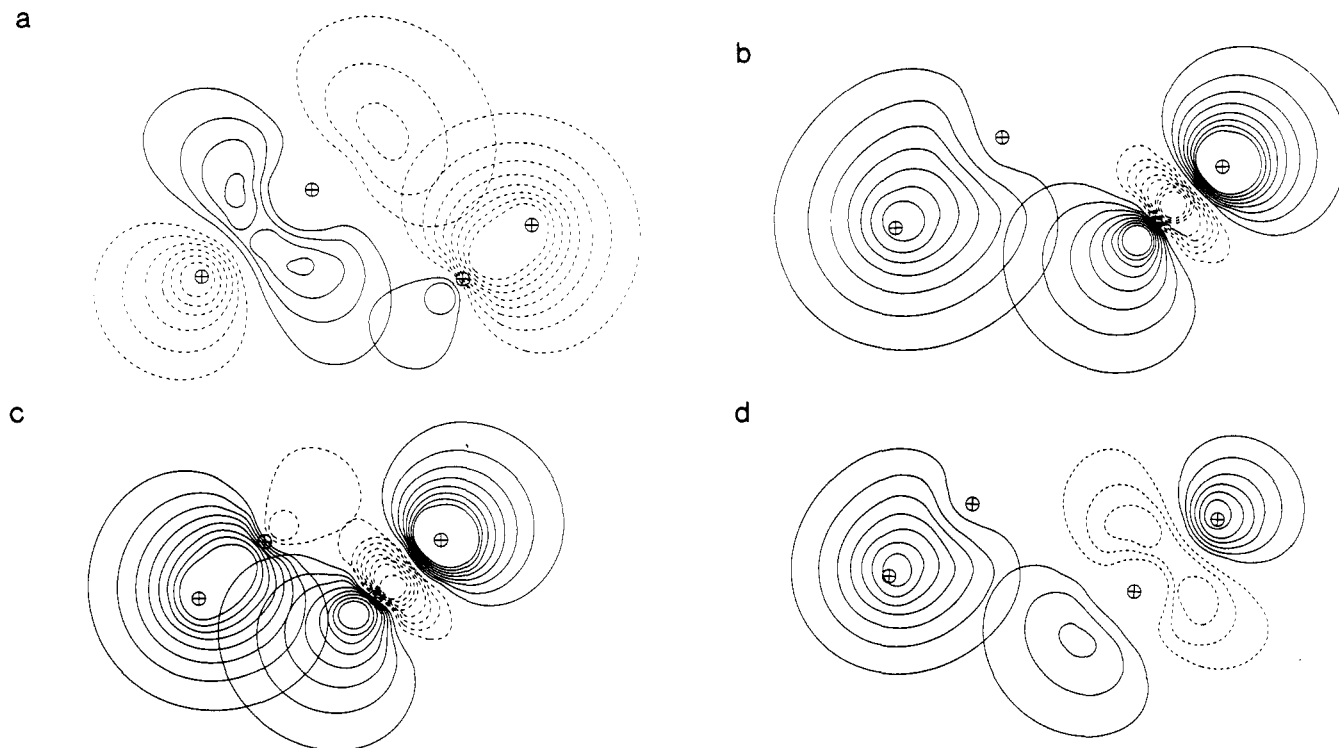
Figure 2. Contour plots (cf. ref 26) of vicinal σX–H→σ*Y–H nonorthogonal natural bond orbitals (NONBO) overlap in staggered H_3X–YH_3 molecules. Projection on the plane defined by X, Y and two antiperiplanar hydrogens. In all cases the same contour spacing has been employed. The valence pseudoorbitals exhibit no radial nodes. (a) σCH (right side), σ*SnH (left side), for H_3C–SnH_3; (b) σSnH (left side), σ*CH (right side), for H_3C–SnH_3; (c) σCH (left side), σ*CH (right side), for ethane; (d) σSnH (left side), σ*SnH (right side), for distannane.

contributions exceed those for the lighter homologues (except for ethane). Comparisons with nonrelativistic pseudopotential calculations (cf. last rows in Tables IV and V) indicate the enhanced vicinal delocalization contributions to be due to the relativistic bond length contraction (cf. section A). The delocalization contributions obtained nonrelativistically fit well into the trend for the lighter homologues. On these bases, one might expect the rotational barrier to be increased significantly by relativistic effects. This is not the case. The differences in the net contributions for the two conformers as well as the calculated rotational barriers do not change at the relativistic level; the increase in overlap influences the stability of the two conformers to the same extent. In particular, contributions from vicinal bonds and antibonds with a dihedral angle of 120° in the eclipsed structure are also larger in the relativistic case. Therefore, relativistic effects for lead compounds do not interrupt the trend to lower and lower barriers for the heavier ethane homologs.

D. Comparative Study of Geometries and Rotational Barriers for Disilane, Hexamethyldisilane, Ethane, and Hexamethylethane. The rotational barrier calculated by Profeta et al.[15] for hexamethyldisilane (1.04 kcal/mol) is remarkably similar to that of the unsubstituted disilane (0.90 kcal/mol). Our results, which were obtained employing larger basis sets and including electron correlation, support this conclusion. Tables VI and VII compare the equilibrium geometries and rotational barriers for disilane, hexamethyldisilane, ethane, and hexamethylethane at different levels of theory,[19] from 3-21G(*) to MP2/6-31G*//6-31G*. Both improvement of the basis set in the Hartree–Fock calculations from 3-21G(*) to 6-31G* and the inclusion of electron correlation corrections (MP2) change the barriers for disilane and for hexamethyldisilane by less than 0.15 kcal/mol (cf. Table VI). The barriers of the two species are almost identical. This is quite different from the situation for ethane vs hexamethylethane. The barrier in the latter (ca. 8 kcal/mol)[36] is considerably larger than the ca. 3 kcal/mol observed for ethane (Table VII). The absolute effect of correlation on the rotational barrier in hexamethylethane (ca. 0.6 kcal/mol) is larger than observed for the disilanes and

(36) Schäfer, L.; Siam, K.; Ewbank, J. D. *Theochem* **1989**, *57*, 111.

Table VI. Comparison of Bond Lengths (Å) and Rotational Barriers, E_{rot} (kcal/mol), of Disilane and Hexamethyldisilane (Staggered and Eclipsed)

(a) Si_2H_6[a]

| level | D_{3d} | | D_{3h} | | |
	Si–Si	Si–H	Si–Si	Si–H	E_{rot}
3-21G(*)//3-21G(*)	2.342	1.478	2.352	1.477	0.90
6-31G*//6-31G*	2.352	1.478	2.362	1.478	0.95
MP2/6-31G*//6-31G*					1.06
exp[b]	2.331 (3)	1.492 (3)			

(b) Si_2Me_6[c]

| level | D_{3d} | | D_{3h} | | |
	Si–Si	Si–C	Si–Si	Si–C	E_{rot}
3-21G(*)//3-21G(*)[d]	2.350	1.897	2.365	1.897	1.04
6-31G*//6-31G*	2.370	1.902	2.382	1.902	0.96
MP2/6-31G*//6-31G*					1.05
exp[e]	2.340 (3)	1.877 (3)			

[a] The bond angles for Si_2H_6 do not vary more than 0.1° at different levels. Geometry at //MP2/6-31G**: Si–Si = 2.334 Å, Si–H = 1.476 Å, H–Si–Si = 110.4°, H–Si–H = 108.6° (D_{3d}); E_{rot} = 1.111 kcal/mol. The experimental angles are H–Si–Si 110.3 (4)° and H–Si–H = 108.6 (4)° (cf. ref 18). Higher-level single-point calculations do not alter the barrier appreciably (e.g., MP4SDTQ/6-31G**// MP2/6-31G**: E_{rot} = 1.067 kcal/mol, E_{tot} = –581.55938 au in D_{3d}). Cf. ref 19 for some of the lower level results. [b] Cf. ref 18. [c] Bond angles for Si_2Me_6 at //6-31G*: C–Si–Si = 110.5°, C–Si–C = 108.5° (D_{3d}); C–Si–Si = 110.7°, C–Si–C = 108.2° (D_{3h}). Attempted optimization of a distorted (D_3) structure at the 3-21G(*) level of theory leads to an essentially D_{3d}-symmetric structure. The experimental angles are C–Si–Si = 108.4°, C–Si–C = 110.5 (4)° (see ref 34). [d] Results of Profeta et al. (see ref 15). [e] Cf. ref 34.

for ethane. However, this is a minor contribution to the high barrier. Steric effects due to methyl substitution have a large effect on the C–C single bond rotational barrier in ethane derivatives.[17] Obviously, these are unimportant for hexamethyldisilane. The hyperconjugative effects discussed in the preceding section depend on the donor and acceptor abilities of vicinal bonds and antibonds.

Table VII. Comparison of Bond Lengths (Å) and Rotational Barriers, E_{rot} (kcal/mol), of Ethane and Hexamethylethane (Staggered and Eclipsed)

	$C_2H_6^a$				
	D_{3d}		D_{3h}		
level	C–C	C–H	C–C	C–H	E_{rot}
3-21G//3-21G	1.542	1.084	1.557	1.083	2.75
6-31G*//6-31G*	1.527	1.085	1.541	1.084	2.99
MP2/6-31G*//6-31G*					3.15
exp	1.531				2.9

	$C_2Me_6^b$				
	D_{3d}		D_{3h}		
level	C–C	C–Me	C–C	C–Me	E_{rot}
3-21G//3-21G	1.578	1.548	1.613	1.549	8.13
6-31G*//6-31G*	1.583	1.542	1.616	1.543	8.00
MP2/6-31G*//6-31G*					8.57
exp^c	1.583 (10)	1.542 (2)			

^{a}Cf. ref 19. ^{b}Bond angles for C_2Me_6 at //6-31G*: Me–C–C = 111.8°, Me–C–Me = 107.0° (D_{3d}); Me–C–C = 112.6°, Me–C–Me = 106.2° (D_{3h}). The energy of a D_3 conformer optimized at 3-21G is 0.3 kcal/mol lower than that of the D_{3d} conformer (D_3, //3-21G: C–C = 1.576 Å, C–Me = 1.547 Å, Me–C–C = 111.5°, Me–C–Me = 107.4°, twist angle = 163.4°). The experimental values are C–C = 1.583 (10) Å, C–Me = 1.542 (2) Å, Me–C–C = 111.0 (0.3)° (see ref 35). ^{c}Cf. reference 35.

In this respect, Si–C(methyl) bonds are similar to Si–H bonds. Hence, the small influence of methyl substitution on the barrier in disilane.

Conclusions

Pseudopotential calculations are convenient for computing the structures and rotational barriers of compounds containing heavy group 14 elements. Relativistic effects, which become important for the lead species, can also be included in the pseudopotential treatment quite effectively.

The rotational barriers of the group 14 ethane congeners decrease with the heavier elements but do not vanish even in H₃-Pb–PbH₃. As noted before for ethane,[6,7,10,26] natural bond orbital analysis indicates that stabilizing vicinal $\sigma X–H \rightarrow \sigma^* Y–H$ delocalization, which stabilizes the staggered conformation, is responsible for the barriers. Poorer overlap as well as smaller orientational dependence of the overlap due to the more diffuse and polarized orbitals involved are the reasons for the decreased barriers in the heavier species. Relativistic bond contraction for the lead compounds increases the individual delocalization contributions but has no net effect on the barrier heights. Hence, the barrier heights of H₃X–YH₃ compounds tend to decrease smoothly down the group 14 set of elements (Figure 1).

Our results for hexamethyldisilane (1) and disilane confirm the interesting observation of Mislow et al.[12] and of Profeta et al.[15] that the rotational barriers for these two species are almost the same. This is due to the absence of significant steric effects and to the similar hyperconjugative donor and acceptor abilities of Si–H and Si–C(alkyl) bonds and antibonds. Thus, methyl and similar substituents probably will not influence the barriers of species involving Ge, Sn, and Pb. The rotational barriers presented in Table I may therefore serve as predictions for many substituted derivatives.

Supplementary Material Available: Table of H–X–Y angles for H₃X–YH₃ (X, Y = C, Si, Ge, Sn, Pb), calculated by using the pseudopotential approach (1 page). Ordering information is given on any current masthead page.